

Dark Energy Survey White Paper for the Dark Energy Task Force

Submitted June 15, 2005

Overview: We plan to carry out a deep optical-near infrared survey of 5000 sq. deg of the South Galactic Cap to $\sim 24^{\text{th}}$ magnitude in SDSS *griz*, using DECam, a new 3 deg² CCD camera to be mounted on the Blanco 4-m telescope at CTIO. The survey data will allow us to measure the dark energy and dark matter densities and the dark energy equation of state through four independent methods: galaxy clusters, weak gravitational lensing tomography, galaxy angular clustering, and supernova distances. These methods are doubly complementary: they constrain different combinations of cosmological model parameters and are subject to different systematic errors. By deriving the four sets of measurements from the same data set with a common analysis framework, we will obtain important cross checks of the systematic errors and thereby make a substantial and robust advance in the precision of dark energy measurements.

DES Collaboration Institutions and Senior Personnel

Fermilab: J. Annis, H. T. Diehl, S. Dodelson, J. Estrada, B. Flaugher, J. Frieman, S. Kent, H. Lin, P. Limon, K. W. Merritt, J. Peoples, V. Scarpine, A. Stebbins, C. Stoughton, D. Tucker, W. Wester.

University of Illinois at Urbana-Champaign: C. Beldica, R. Brunner, I. Karliner, J. Mohr, R. Plante, P. Ricker, M. Selen, J. Thaler

University of Chicago: J. Carlstrom, S. Dodelson, J. Frieman, M. Gladders*, W. Hu, E. Sheldon, R. Wechsler. * Carnegie Observatories until summer 2006

Lawrence Berkeley National Lab: G. Aldering, N. Roe, M. Levi, S. Perlmutter

NOAO/CTIO: T. Abbott, C. Miller, C. Smith, N. Suntzeff, A. Walker

Institut d'Estudis Espacials de Catalunya: F. Castander, P. Fosalba, E. Gaztañaga, J. Miralda-Escude

Institut de Fisica d'Altes Energies: E. Fernández, M. Martínez

University College London: O. Lahav, P. Doel, M. Barlow, R. Bingham, S. Bridle, S. Viti, J. Weller

University of Cambridge: G. Efstathiou, R. McMahon, W. Sutherland

University of Edinburgh: J. Peacock

University of Portsmouth: R. Nichol

University of Michigan: R. Bernstein, A. Evrard, D. Gerdes, T. McKay

Background: The National Optical Astronomy Observatory (NOAO) issued an announcement of opportunity (AO) in December 2003 for an open competition to partner with NOAO in building an advanced instrument for the Blanco telescope in exchange for awarding the instrument collaboration up to 30% of the observing time over a five-year period for a compelling science project. In response to this AO, we formed the Dark Energy Survey (DES) Collaboration to build DECam with the goal of addressing the nature of the dark energy. We submitted our proposal to NOAO in July 2004 and after reviewing our proposal NOAO concluded that our scientific goals are exciting and timely. Subsequently, the NOAO Director asked the CTIO Director and the DES Project Director to draft a MOU among the Parties that would define the terms of the partnership.

Dark Energy Survey Techniques: Here we present a brief summary of the four proposed techniques. The resulting dark energy constraints are described in the following section. We describe these techniques and their associated uncertainties in greater detail in **The Supplements for the Dark Energy Survey**.

Galaxy clusters: The evolution of the galaxy cluster mass function and cluster spatial correlations provide a sensitive probe of the dark energy; these observables are affected by cosmology through both the growth of density perturbations and the evolution of the volume element (Haiman, Mohr, & Holder 2000, Battye & Weller 2003). Clusters make promising cosmological probes, because the formation of these large potential wells involves only the gravitational dynamics of dark matter to good approximation. The primary design driver of the DES is the detailed optical measurement of galaxy clusters, including photometric redshifts, in conjunction with the South Pole Telescope (SPT) Survey. The SPT will use the Sunyaev-Zel'dovich effect (SZE) to detect galaxy clusters out to large distances, providing a census of

tens of thousands of clusters over a 4000 square degree region south of declination $\delta = -30^\circ$. The SZE signal is expected to be a robust indicator of cluster mass, because it is a measure of the thermal energy of the electrons residing in the gravitational potential well. The DES is designed to measure efficiently and accurately photometric redshifts for all SPT clusters to $z=1.3$. It will also cross-check the completeness of the SPT cluster selection function by optically identifying clusters below the SPT mass threshold and will statistically calibrate SZE cluster mass estimates using the cluster-mass correlation function inferred from weak lensing. Existing cameras would require decades to cover the SPT survey area to the requisite depth.

Weak lensing tomography: The DES will measure the weak lensing (WL) shear of galaxies as a function of photometric redshift. The evolution of the statistical pattern of WL distortions—for example, the shear-shear (S-S) angular power spectrum—and of the cross-correlation between foreground galaxies and background galaxy shear (galaxy-shear correlations, G-S), are sensitive to the cosmic expansion history through both geometry and the growth rate of structure (Hu 2002, Huterer 2002). In the course of surveying 5000 sq. deg. to the depth required for cluster photo- z 's, the DES will measure shapes and photometric redshifts for ~ 300 million galaxies and, with improved control of the optical image quality, enable accurate measurement of lensing by large-scale structure.

Galaxy angular clustering: The DES will measure the angular clustering of galaxies (denoted G-G in Table 1) in photometric redshift shells out to $z\sim 1.1$. The matter power spectrum as a function of wavenumber shows characteristic features, a broad peak as well as baryon wiggles arising from the same acoustic oscillations that give rise to the Doppler peaks in the CMB power spectrum; these features were recently detected in the SDSS (Eisenstein et al 2005). In combination with CMB observations, they serve as standard rulers for distance measurements, providing a geometric test of cosmological parameters. This approach will provide cosmological information from the shape of the power spectrum transfer function and physically calibrated distance measurements to each redshift shell (e.g., Hu & Haiman 2003, Seo & Eisenstein 2003, Blake & Bridle 2004).

Supernova luminosity distances: In addition to the wide-area survey, the DES will use 10% of its allocated time to discover and measure well-sampled *riz* light curves for ~ 1900 Type Ia supernovae in the redshift range $0.3 < z < 0.75$ through repeat imaging of a 40 deg^2 region. These SNe will provide relative distance estimates to constrain the properties of the dark energy.

In addition to these methods, cross-correlation of CMB data sets with DES galaxies as tracers of potential wells will probe the dark energy through the integrated Sachs-Wolfe (ISW) effect; this effect is included in the forecast constraints below (Hu & Scranton 2004). Finally, we note that accurate photometric redshifts are critical to the DES science goals; as a relatively shallow survey, a major advantage of the DES will be the availability of spectroscopic redshift calibration (training) samples that extend out to the flux limit of the survey.

Forecast Dark Energy Constraints: In this section, we quantify how the DES will improve our understanding of dark energy, focusing on the dark energy equation of state parameter w . Such forecasts generally depend upon priors assumed for marginalized parameters and on assumptions about whether w evolves. The marginalized parameters include cosmological parameters other than w , uncertain astrophysical parameters that characterize a particular probe, and possible parameters describing uncorrected systematic errors associated with a particular observational method. As a result, caution must be exercised in comparing the projected dark energy sensitivity of different methods and experiments. For this discussion, we assume constant w and consider 3 cases of cosmological priors: uniform, present CMB (WMAP 1-year), and future CMB (Planck); these priors are specified in The Supplements. While models with constant $w \neq -1$ are not theoretically well motivated, they nevertheless provide a convenient metric for comparison. A few examples of forecasts with time-varying w are discussed in The Supplements. We

also note that for varying w , for the redshift z_p at which $w(z)$ is best constrained, the constraints on $w(z_p)$ are the same as those on constant w shown below.

Table 1: Example forecast marginalized 68% CL statistical DES constraints on constant equation of state parameter w .

Method/Prior	Uniform	WMAP	Planck
Clusters:			
abundance	0.13	0.10	0.04
w/ WL mass calibration	0.09	0.08	0.02
Weak Lensing:			
Shear-shear (S-S)	0.15	0.05	0.04
Galaxy-shear(G-S)+G-G	0.08	0.05	0.03
S-S+G-S+G-G	0.03	0.03	0.02
S-S+bispectrum	0.07	0.03	0.03
Galaxy angular clustering	0.36	0.20	0.11
Supernovae Ia	0.34	0.15	0.04

In all cases considered in Table 1, we assume cold dark matter, negligible neutrino masses, adiabatic Gaussian initial perturbations with power-law primordial power spectrum, and a spatially flat Universe. We use a fiducial model with $w = -1$ and other parameters close to the WMAP concordance values. Further assumptions for each method are given in the remainder of this section. The numbers in Table 1 can change as those assumptions are varied within reasonable limits and are meant to be representative. These numbers, based on Fisher matrix and Monte Carlo analyses, indicate that each of the four methods can probe constant w with *statistical* errors at the 3-20% (2-11%) level for WMAP (Planck) priors, assuming reasonable uncertainties in the appropriate astrophysical parameters as noted in the remainder of this section. In fact, we expect these methods will likely be limited by systematic errors. A description of their expected impact on the cosmological parameter error budget is presented in The Supplements.

For the cluster results, we have used the cluster counts above the 5σ SPT detection limit (1.9mJy, with a beam of 1' FWHM) in redshift bins of $\Delta z=0.1$ out to $z=1.5$, which results in $\sim 12,000$ clusters over 4000 deg^2 for the fiducial cosmology and a weakly redshift-dependent mass threshold of $\sim 2 \times 10^{14} M_{\text{sun}}$. The SZE detection threshold was set this high (as opposed to, say, 3σ) in order to minimize the effects of sample contamination by radio point sources. We have marginalized over a 3-parameter model for the mass-SZE flux relation that includes power-law evolution with redshift, but no scatter in that relation. While this mass-SZE flux relation is rather simple, there is additional information contained in the cluster angular power spectrum and in the shape of the mass function (rather than just its integral above a threshold) that can be used to help "self-calibrate" a more complex relation (Majumdar & Mohr 2004, Lima & Hu 2004, 2005). Moreover, the second row of cluster constraints in Table 1, includes the statistical calibration of the mass-observable relation using the cluster-shear cross-correlation over the mass range $4 \times 10^{14} - 2 \times 10^{15} M_{\text{sun}}$ in redshift bins from $z=0.4-0.9$. Finally, we have assumed that the theoretical uncertainties in the halo mass function, in the halo bias as a function of mass, and in the identification of SZE-detected clusters with dark halos are subdominant compared to the other errors; recent N-body simulations indicate that the first two assumptions are justified and planned future simulations will be needed to ensure the third.

The forecast weak lensing constraints assume that the shear and galaxy power spectra are each measured in 5 photometric redshift bins out to $z=2$ (for background galaxy shear) and $z=1$ (for foreground galaxy positions), with a simplified but reasonable model for the photo- z errors, $\sigma(z)=0.05(1+z)$. The statistical errors come from cosmic variance and from shot noise (shape noise) corresponding to an effective

background density of 10 galaxies/arcmin² (with shape noise per shear component of 0.16); artificially degrading higher resolution images yields this source density for the DES depth and the 0.9" median seeing delivered by the Mosaic II Camera on the Blanco. If the delivered seeing can be reduced to ~0.7", close to the median site seeing for the DES observing months, the effective background density will increase by ~35%, with the shot noise errors in the shear-shear power spectrum correspondingly reduced. The results in Table 1 use angular information and assume Gaussian errors up to multipoles $l < 1000$, beyond which non-linearities in the density field become important at the typical survey depth; a more conservative (aggressive) limit of $l = 300$ ($l = 3000$) increases (decreases) the w constraints by ~50%. In these forecasts, the non-linear mass power spectrum is modeled by the halo model (Hu & Jain 2004), which reproduces the results of high-resolution N-body simulations. For constraints that include foreground galaxies (i.e., G-G and G-S), 5 halo occupation parameters per foreground galaxy photo-z bin are marginalized over. These parameterize the bias of galaxies with respect to the dark matter in a manner consistent with high-resolution N-body simulations (Kravtsov et al 2004) and with the observed clustering of galaxies at low redshift in the SDSS (Zehavi et al 2004). For constraints including (G-G), the foreground galaxy power spectrum is only used to provide constraints on these halo occupation parameters.

The galaxy angular clustering constraint assumes measurement of the angular power spectrum for the foreground galaxy sample with photo-z binning and errors as above. However, it uses a more conservative range of angular information, $l < 300$, since baryon wiggles are washed out in the non-linear regime; compared to the first two methods, this result is more robust to uncertainties in non-linear perturbation evolution. Since this clustering constraint mainly uses the shape of the power spectrum, it is not very sensitive to the galaxy bias model. As a result, its use here is complementary to its use above in constraining galaxy bias for lensing.

The forecast supernova constraints assume SNe Ia are standardizable candles with an intrinsic dispersion in peak luminosity of 0.25 mag; this is larger than the usually adopted value of 0.15 mag and reflects an expected increase in errors due to the fact that only photometric redshifts will be available for the majority of the sample. These constraints also assume an irreducible systematic error floor in peak magnitude dispersion of $0.02(1+z)/1.8$ mag in redshift bins of $\Delta z = 0.1$ (e.g., Frieman et al 2003). Under this assumption, the error floor dominates over the intrinsic dispersion in the derived dark energy constraints, so there is little gain from reducing the intrinsic dispersion; with no systematic error floor, the w constraints improve to 0.24, 0.14, and 0.03 for uniform, WMAP, and Planck priors. In all cases, we have also assumed a well-measured set of 300 nearby ($z < 0.1$) SNe Ia (being accumulated by on-going surveys) anchors the low-redshift part of the Hubble diagram.

Systematic Errors: Table 2 lists the expected dominant systematic error sources for each method, ordered approximately from most to least important, along with the presently envisioned primary methods for controlling them. A more detailed discussion is presented in The Supplements.

For the cluster technique, the cluster sample must be both complete (above some threshold) and free of contamination, i.e., the cluster selection function must be well understood. For the SZE, cluster selection is complicated by point source confusion, dusty galaxies, radio galaxies, primary CMB anisotropy, and chance projection of clusters at different redshifts. The systematics for DES optical cluster selection are quite different, so the two methods can be compared to understand the selection function. Prior to SPT, the SZA (now operational) will carry out deep SZE imaging over a smaller area of sky with higher angular resolution; this will provide improved calibration of the mass-SZE flux relation and probe the SZE selection function below the SPT threshold. Prior to DES, members of our collaboration will carry out a 100 sq. deg. multi-band imaging survey with Mosaic II on the Blanco (recently approved as a 3-year survey program beginning in Fall 2005) that overlaps several planned SZE surveys (including APEX, ACT, and SPT); this survey will enable cross-comparison of the SZE and optical cluster selection functions for a fraction of the sample. In addition, we will quantify the SZE cluster selection function

through a program of hydrodynamic simulations (Melin et al 2004, Vale & White 2005) and Monte Carlo simulations based on radio source catalogs to evaluate contamination. The cluster technique also relies on an accurate mass-observable relation; as noted above, this will be calibrated by statistical weak lensing, the cluster angular power spectrum, and the shape of the cluster mass function.

Table 2: Dominant sources of systematic error and methods for controlling them; see text.

Method	Dominant Systematic Errors	Primary Controls
Clusters	Sample selection Mass-observable relation	SZE + optical cluster selection; simulations Self-calibration; statistical WL masses
Weak Lensing	Multiplicative shear Additive shear Photo-z biases Small-scale power spectrum	Measurement algorithm; shear vs. gal. size PCA; active focus; wave-front sensing & alignment control Spectroscopic calibration sets Null small-scale power; high-res. simulations
Angular clustering	Bias prescription errors Large-scale photometric calibration errors Photo-z biases	Angular bispectrum; clustering by type Calibration strategy; clustering by color; angular sub samples Spectroscopic calibration sets
Supernovae Ia	SN evolution Photometric errors Extinction Photo-z errors & biases	Low and high z SNe comparison Calibration strategy; artificial SNe SN color and host galaxy information SN spectroscopic calib. sub sample

For weak lensing, the dominant systematic errors are additive and multiplicative shear systematics (Huterer, Takada, Bernstein, & Jain 2005, hereafter HTBJ), uncorrected biases in photo-z estimates (HTBJ 2005; Ma, Hu, & Huterer 2005), and theoretical uncertainties in the small-scale mass power spectrum (White 2004, Zhan & Knox 2004, Huterer & Takada 2004). Theoretical uncertainties can be controlled by nulling the small-scale information (Huterer & White 2005) and by using improved high-resolution N-body simulations incorporating baryons. Photo-z biases will be controlled to an acceptable level by using a pre-existing spectroscopic redshift sample large and deep enough to accurately determine the photo-z error distribution as a function of redshift. The Supplements summarize the acceptable error budget for additive and multiplicative shear systematics (HTBJ) and the techniques we will pursue to reduce them to acceptable levels.

For angular clustering, the dominant systematic errors are potential inadequacy of the halo occupation description of galaxy bias (affecting the baryon wiggles), photometric calibration errors or uncorrected Galactic dust extinction correlated over large scales (leading to artificial large-scale power), and photo-z biases. Since the angular bispectrum and power spectrum have different dependences on the galaxy bias parameters, combining them will constrain those uncertainties (Dolney et al 2004, Gaztanaga & Frieman 1996). In addition, since galaxy bias depends on galaxy type (color and luminosity) measuring angular clustering for different types will constrain the large-scale behavior of the bias. Correlated photometric errors will be controlled by a survey strategy that incorporates multiple visits to each field, by clustering vs. galaxy color, and by checking consistency of results across different angular sub samples.

For supernovae, the major systematic errors are evolution of the supernova population, systematic photometric errors, uncorrected host-galaxy extinction, inaccurate K-corrections, and photo-z errors and biases for the part of the sample without spectroscopic redshifts. Evolution is generally controlled by comparing light-curves, colors, and spectra of high- and low-z supernovae and using the fact that the low-z sample, if large enough, should span the range of physical conditions encountered in the sample to $z \sim 1$. Photometric errors will be minimized by a survey strategy optimized for uniform calibration and cross-

checked by overlap with SDSS photometry on the celestial equator. K-correction uncertainties will be mitigated by having a large, nearby comparison SN sample with multi-epoch spectrophotometry. Extinction errors will be addressed by using host galaxy colors to identify a low-extinction sub sample of early-type galaxies. The impact of photo-z errors is discussed in The Supplements and is expected to be small.

Dark Energy Survey Baseline Proposal: We have requested 525 nights over 5 years, concentrated between September and February, and with that time expect to reach photometric limits of $g=24.6$, $r=24.1$, $i=24.3$, and $z=23.9$ over 5000 sq. deg. These are 10σ limits in $1.5''$ apertures assuming $0.9''$ seeing and are appropriate for faint galaxies; the corresponding 5σ limit for point sources is 1.5 mags fainter. These limits are derived from detailed survey simulations that incorporate weather data at CTIO over a 30-year baseline. The survey strategy is designed to optimize the photometric calibration by tiling each region of the survey with at least four overlapping pointings in each band. This provides uniformity of coverage and control of systematic photometric errors via relative photometry on scales up to the survey size. This strategy will enable us to determine photometric redshifts of galaxies to an accuracy of $\sigma(z)\sim 0.07$ out to $z>1$, with some dependence on redshift and galaxy type, and cluster photometric redshifts to $\sigma(z)\sim 0.02$ or better out to $z\sim 1.3$, both sufficient to meet the science requirements. 4000 deg^2 of the survey region will overlap the SPT survey region; the remainder will provide coverage of spectroscopic redshift training sets, including the SDSS southern equatorial stripe, and more complete coverage near the South Galactic pole. The details of the baseline supernova survey are given in The Supplements.

Precursor and Concurrent Observations and Developments:

1. Spectroscopic redshift data sets to the DES flux limit to calibrate empirical photo-z estimators, to measure photo-z error distributions, and to provide a sample of SN host galaxy redshifts. These will be in place prior to DES from on-going surveys (including SDSS, 2dFGRS, VIMOS VLT Deep Survey, and DEEP2). The overlap of DES with a planned VISTA NIR survey will improve galaxy photo-z estimates but is not required to satisfy the DES science requirements.
2. The SPT survey for SZE measurements of galaxy clusters. SPT and DES plan joint analyses. SPT, which will start survey operations in 2007, expects to have 1-2 years of survey data by the time DES starts operations. A precursor 100 deg^2 survey with Mosaic II commencing fall 2005 will overlap several planned SZE surveys, including SPT, and help constrain the cluster selection function.
3. Follow-up spectroscopy of a subsample of $\sim 25\%$ of the SNe Ia on 8m-class telescopes, relying primarily on competitive time applications in collaboration with the supernova community. This will use 8m-class resources at a rate comparable to or less than current high-z SN follow-up; it will reduce cosmological errors from and test the purity of the SN sample. A low-redshift sample of well-measured SNe Ia to anchor the Hubble diagram and provide spectroscopic and photometric templates for SN light-curve fitting and K-corrections; this will be done by ongoing surveys (KAIT, CSP, SDSS-II, SNF).
4. Suites of large N-body simulations incorporating hydrodynamics by collaboration members to precisely calibrate the theoretical cluster mass function and better model SZE and optical cluster selection. Simulations will also determine with greater precision the effects of clustering non-linearity and baryons on weak lensing and galaxy angular clustering.

DECam, the Survey Instrument: The philosophy of the DECam project is to assemble proven technologies into a powerful survey instrument and mount the instrument on an optimally configured Blanco, thereby exploiting an excellent, existing facility. Figure 1 shows a cross section of DECam with the key elements identified. A discussion of the Blanco performance and upgrades are given in the The Supplements.

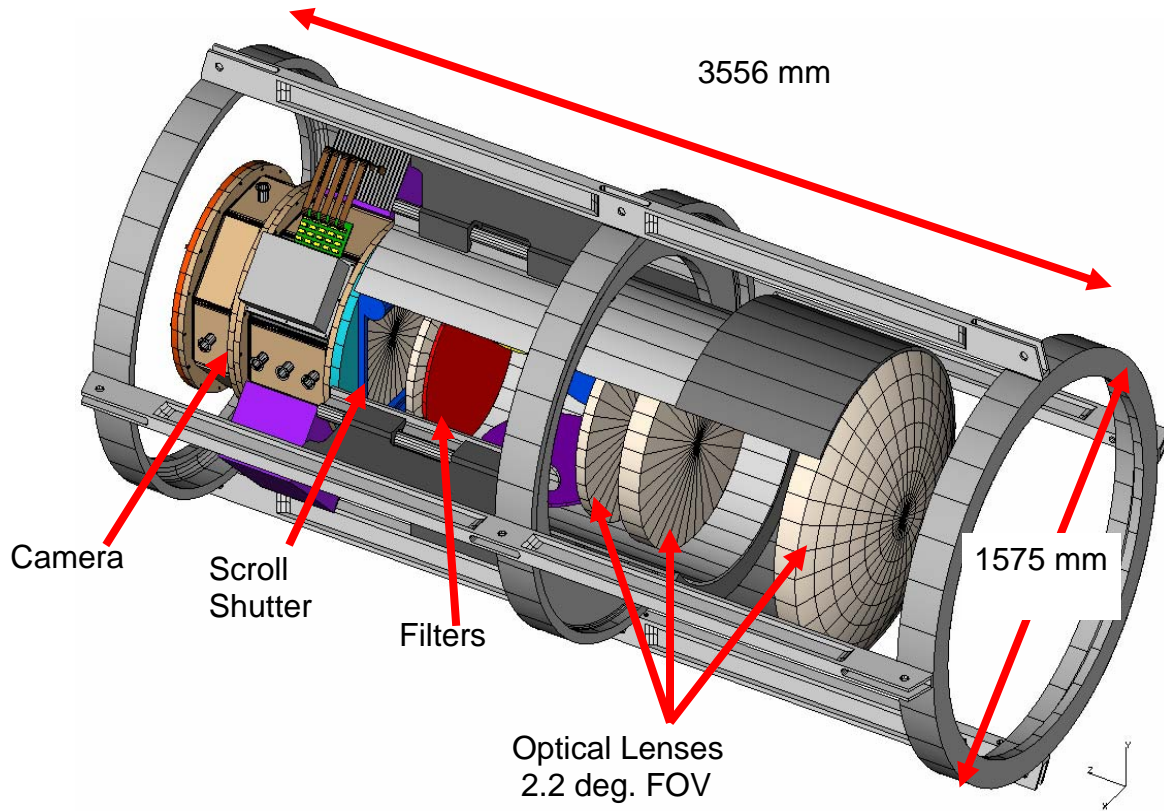


Figure 1: DECam Reference Design

The major components of DECam are a 519 megapixel optical CCD camera, a wide-field optical corrector (2.2 deg. field of view), a 4-band filter system with SDSS *g r i* and *z* filters, guide and focus sensors mounted on the focal plane, low noise CCD readout, a cryogenic cooling system to maintain the focal plane at 180 K as well as a data acquisition and instrument control system to connect to the Blanco observatory infrastructure. The camera focal plane will consist of sixty-two 2k x 4k CCDs (0.27"/pixel) arranged in a hexagon covering an imaging area of 3 sq. degrees. Smaller format CCDs for guiding and focusing will be located at the edges of the focal plane. To efficiently obtain *z*-band images for high-redshift ($z \sim 1$) galaxies, we have selected the fully depleted, high-resistivity, 250 micron thick silicon devices that were designed and developed at the Lawrence Berkeley National Laboratory (LBNL) (Holland et al. 2003). The thickness of the LBNL design has two important implications for DES: fringing is eliminated, and the QE of these devices is $> 50\%$ in the *z* band, a factor of ~ 10 higher than traditional thinned astronomical devices. Several of the LBNL 2k x 4k CCDs of this design have been successfully used on telescopes, including the Mayall 4m at Kitt Peak and the Shane 3m at Lick. The DES CCDs will be packaged and tested at Fermilab, capitalizing on the experience and infrastructure associated with construction of silicon strip detectors for the Fermilab Tevatron program. The CCD packaging plan for the four side buttable 2k x 4k devices builds on techniques developed by LBNL and Lick Observatory.

The optical corrector reference design consists of five fused silica lenses that produce an unvignetted 2.2° diameter image area, which is calculated to contribute $< 0.4''$ FWHM to the point-spread function. Element 1, the largest, is 1.1m in diameter and the surface of another is aspheric. The spacing between elements 3 and 4 will allow the 600 mm diameter filters to be individually flipped in and out of the optical path. DECam will be installed in a new prime focus cage.

Table 3: Expected performance of DECam, Blanco, and CTIO site

Blanco Effective Aperture/ f number @ prime focus	4 m/ 2.7
Blanco Primary Mirror - 80% encircled energy	0.25 arcsec
Optical Corrector Field of View	2.2 deg.
Wavelength Sensitivity	400-1100 nm
Filters	SDSS g, r, i, z
Effective Area of CCD Focal Plane	3.0 sq. deg.
Image CCD pixel format/ total # pixels	2k X 4k/ 519 Mpix
Guide, Focus & Wavefront Sensor CCD pixel format	2k X 2k
Pixel Size	0.27 arcsec/ 15 μ m
Readout Speed/Noise goal	250 kpix/sec/ 5 e
DECam Corrector (Reference Design) 80% encircled energy (center/edge)	g (0.32/0.59 arcsec) r (0.11/0.37 arcsec) i (0.17/0.41 arcsec) z (0.31/0.47 arcsec)
Survey Area	5,000 sq. deg.
Survey Time/Duration	525/5 (nights/years)
Median Site Seeing Sept. – Feb.	0.65 arcsec
Median Delivered Seeing with Mosaic II on the Blanco	0.9-1.0 arcsec (V band)
Limiting Magnitude: 10σ in 1.5" aperture assuming 0.9" seeing, AB system	g=24.6, r=24.1, i=24.3, z=23.9
Limiting Magnitude: 5σ for point sources assuming 0.9" seeing, AB system	g=26.1, r=25.6, i=25.8, z=25.4

A Fermilab Director's Review (June 2004) and an NOAO Blanco Instrumentation Panel Review (August 2004) evaluated DECam, and both reviews identified the yield of the CCDs, the front end electronics (FEE), and the large optics as the major risks to the project cost and schedule. We have focused our R&D efforts on the mitigation of these risks. The Supplements present further details of the R&D program. In particular, we adopted a proven CCD device design and placed the first DES CCD wafer order. The first test devices were delivered to LBNL in early June 2005 and have been successfully read out on cold probe station. We anticipate delivery of the first thinned fully processed devices this fall. The production of the DES devices by LBNL provides an excellent precursor to the production of devices for the SNAP/JDEM project.

To benefit from the on-going development at NOAO, we have adopted the Monsoon CCD readout system as a starting point. UIUC and Fermilab each have a Monsoon system and are preparing to read out LBNL CCDs in the near future. As we gain experience with Monsoon in the testing setups, we will build on the design and make the modifications necessary to meet the prime focus cage space and heat restrictions.

The risks associated with the optical design result from the size of the elements. Since our last review we have added collaborators with extensive experience in designing and procuring optical components. With them we are investigating alternative designs with smaller first elements (~0.9m) and better image quality, with the goal of cost and schedule reduction. We have joined a group organized by George

Jacoby to collaborate on the development of large filters for imaging cameras (WIYN, LSST, PanSTARRS). We are also following the development of large colored glass filters at Schott.

Data Management: The DES data management system (DM) is designed to enable efficient, automated grid processing, quality assurance, and long-term archiving of the ~1 Petabyte DES dataset. The raw and processed data will be archived and, after one year, distributed to the public. The survey data will move from CTIO to the National Center for Supercomputing Applications (NCSA) in Illinois, the primary data processing center, over data lines provided by NOAO. The images will be processed, combined into deeper co-added images, and reduced to science-ready data at the catalog level at NCSA. DM is a collaborative effort led by U. Illinois that includes major contributions from Fermilab and the NOAO Data Products Program (DPP). The DM development project will include yearly data challenges that involve testing the system with simulated DES data. Our fourth and final data challenge will end in January 2009, several months before first light for the DES camera.

The DM system includes a pipeline processing environment and data access framework to enable automated and modular processing of this large dataset. This framework will be provided by NCSA and is closely coupled to their large, middleware development effort for the LSST data management project. The DM system includes astronomy modules for processing and data quality assurance, which will come from the collaboration. The primary image archive will employ the NOAO Science Archive software, which is being developed by NOAO DPP. The development of the DES catalog database and server is being led by NCSA.

DES Timeline:

October 2004	Start DECam R&D and continue the preliminary design
April 2006	Hold preliminary design review, obtain DOE project approval, and place long lead procurements with non-DOE funds
October 2006	Place long lead procurements with DOE funds, begin production processing, packaging and testing of CCDs
October 2008	Complete construction of DECam and Data Management System (DM)
February 2009	Deliver DECam and DM to CTIO
May 2009	Begin commissioning of DECam on the Blanco with the completed DM
September 2009	Begin observations
March 2014	Complete observations

Conclusions: The Dark Energy Survey will employ four complementary techniques to study dark energy: galaxy clusters, weak lensing, galaxy angular clustering, and supernova distances. The statistical reach of these techniques is well understood; in the DES, *each* of them will deliver statistical constraints on dark energy that are stronger than the best *combined* constraints available today (Spergel et al 2003, Tegmark et al 2004, Seljak et al 2004). Moreover, our collaboration is making substantial progress toward identifying and understanding the dominant astrophysical uncertainties and observational systematic errors for each of these methods and one of our important goals is to further explore and develop methods to control these systematic errors. Since the more ambitious surveys of the future will reach even smaller statistical errors than the DES, they will have to exercise even finer control of systematic errors in order to achieve their science goals. We believe that a large-scale, near-term survey that provides a major step forward in precision such as DES is the logical next step in that process.

The DES will employ DECam, a powerful new wide-field survey instrument, and the Blanco, a 4m telescope that has already contributed to many of the pioneering measurements of dark energy and that has the capacity for improvements that will strengthen the DES measurements. As a relatively shallow survey, the DES makes use of source galaxies that are large enough to be well resolved in the conditions routinely achieved with MOSAIC II, the current Blanco imager, and bright enough so that their photometric redshifts can be well calibrated by spectroscopic surveys of comparable depth. The

collaboration institutions have a proven record in astronomical data management and have the capacity to manage large data sets. Collaboration members have made important contributions to developing the survey science, and include a strong science team that will rise to the challenge of carrying out the astrophysical and cosmological simulations that will be needed to precisely interpret the data from this large survey. The DES promises significant scientific returns, although it is a relatively low-risk project of intermediate scope and cost, which requires only modest advances beyond the hardware and software used in current astronomical projects.

DES will also provide the astronomical community with a wide field, 4 band digital survey of the southern sky with excellent image quality, uniform photometry and unprecedented depth for its sky coverage. It will cover the largest volume of the universe to date (complete to tens of Gpc³) and it will be a "legacy survey" that will provide the scientific and educational communities with an extraordinary catalog for multipurpose projects.

The DES and the SPT projects provide a unique opportunity to combine two strong surveys into a single survey that will be greater than the sum of its parts. The very strong impact that they can make together on cosmology will be much greater if the observations are made in a timely way. The SPT project will begin observations in 2007, thus it is important for DES to start its build phase soon.

Acknowledgements: The Collaboration recognizes Dragan Huterer, Buvnesh Jain, and Masahiro Takada for their exceptional help in preparing the white paper and The Supplements.

References

- Battye, R.A., & Weller, J. 2003, Phys. Rev. D, 68, 083506
Blake, C., & Bridle, S. 2004, MNRAS, submitted, astro-ph/0411713
Dolney, D., et al. 2004, astro-ph/0409445
Eisenstein, D.J., et al. 2005, ApJ, submitted, astro-ph/0501171
Frieman, J.A., et al. 2003, Phys. Rev. D, 67, 083505
Gaztanaga, E., & Frieman, J.A. 1994, ApJ, 437, L13
Haiman, Z., Mohr, J.J., & Holder, G.P. 2001, ApJ, 553, 545
Holland, S.E., et al. 2003, IEEE Trans. Electron Dev., 50(3), 225
Hu, W. 2002, Phys. Rev. D, 66, 083515
Hu, W., & Haiman, Z. 2003, Phys. Rev. D, 68, 063004
Hu, W., & Jain, B. 2004, Phys. Rev. D, 70, 043009
Hu, W., & Scranton, R. 2004, Phys. Rev. D, 70, 123002
Huterer, D. 2002, Phys. Rev. D, 65, 063001
Huterer, D., & Takada, M. 2005, Astropart. Phys., 23, 369
Huterer, D., Takada, M., Bernstein, G., & Jain, B. 2005, astro-ph/0506030 (HTBJ)
Huterer, D., & White, M. 2005, Phys. Rev. D, submitted, astro-ph/0501451
Kravtsov, A.V., et al. 2004, ApJ, 609, 35
Lima, M., & Hu, W. 2004, Phys. Rev. D, 70, 043504
Lima, M., & Hu, W. 2005, Phys. Rev. D, submitted, astro-ph/0503363
Ma, Z., Hu, W., & Huterer, D. 2005, in preparation
Majumdar, S., & Mohr, J.J. 2004, ApJ, 613, 41
Melin, J.-B., et al. 2005, A&A, 429, 417
Seo, H.-J., & Eisenstein, D.J. 2003, ApJ, 598, 720
Vale, C., & White, M. 2005, New Astronomy, submitted, astro-ph/0501132
White, M. 2004, Astropart. Phys., 22, 211
Zehavi, I., et al. 2004, ApJ, 608, 16
Zhan, H., & Knox, L. 2004, ApJ, 616, 75